Design and Analysis of Miniaturized Multiband High Frequency Antenna for K and Ka Band Applications

P.JOTHILAKSHMI[1#], S.RAJU[1*]
[1#]Department of Electronics and Communication Engineering
Sri Venkateswara College of Engineering, Chennai, Tamilnadu, India
jothi@svce.ac.in
[1*]Department of Electronics and Communication Engineering
Thiagarajar College of Engineering, Madurai, Tamilnadu, India
rajuabhai@tce.edu

Abstract:- This paper proposes the design and analysis of co-axial continuous transverse stub multiband antenna (CCTS) for multiple high frequency Applications. Coaxial continuous transverse stub antenna is used to operate on multiple frequency bands with small size and low cost. This proposed antenna consists of two stubs, arranged longitudinally to form a waveguide skeleton like structure. The advantages of CCTS antenna are used to produce omnidirectional radiation pattern in the horizontal plane. This antenna can radiate for the frequency range of 24.5 GHz to 35 GHz which is suitable for portion of K band and Ka band wireless applications. This proposed structure produces very good radiation pattern in both vertical and horizontal plane with minimum acceptable return loss. The simulation software used in this design is CST Microwave Studio and MATLAB.

Key-Words:- Multiband, Stub, Continuous Transverse Stub, Antenna Array, S-parameter, Radiation Pattern, VSWR.

1 Introduction

Multiband continuous transverse stub (CTS) technology developed in the early 1990s by Hughes Aircraft Company [7], [9] has attracted research attention recently. CTS technology offers greater tunable bandwidth than waveguide or patch antennas. The different forms of CTS antenna include coaxial, coplanar and rectangular waveguide [3], [4], [6], [16]. This structure exhibits a very low Q and impedance characteristics CTS structure offers several advantages over planar CTS. The impedance matching is inherently easier in coaxial structures, providing higher efficiency and facilitates system integration with other coaxial structures. The dominant mode of operation of this CCTS structure is quasi TEM. The CTS element is not only used to construct an antenna, it is used to construct filter, couplers and other microwave components. The proposed antenna structure has operating for four different frequencies which is well suitable for satellite and Radar applications.

2 Basic Theory

Continuous transverse stub structure is a multimode structure and supports number of waveguide modes which simultaneously meet the boundary conditions imposed by the two parallel plates structure. The number of relative intensity of these propagating modes depends on transverse excitation function excited by the finite line source. Once excited, these mode coefficients are unmodified by the presence of the CTS element because of its continuous nature in the transverse plane. In theory [17], [18], each mode has associated with it a unique propagation velocity which, given enough distance, will cause undesirable dispersive variation of the line source imposed excitation function in the longitudinal direction of propagation. However for typical excitation functions, these mode velocities differ from that of the dominant TEM mode by much less than one percent and the transverse plane imposed by the line source is translated, without modification, over the entire finite longitudinal extent of the CTS array structure. Fig.1. shows the various configurations of continuous transverse stub elements used in practice. These structures shows that the stubs are open circuited or short circuited with dielectric depending on the applications. Radiating and reactive CTS elements are available.

A continuous transverse stub element residing in one or both conductive plates [17], [18], [20] of a parallel plate waveguide is employed as a coupling, reactive, or radiating element in microwave, millimeter-wave, and quasi-optical coupler, filter, or

antenna. The most general form of the continuous transverse stub element comprises an antenna that includes the following elements, dielectric element comprising a first portion and a second portion that extends generally transverse to the first portion that forms a transverse stub that protrudes from a first surface of the first portion, first conductive element disposed coextensive with the dielectric element along a second surface of the first portion and second conductive element disposed along the first surface of the dielectric element and disposed along transversely extending edge walls formed by the second portion of the dielectric element. The numerous other variations of the transverse stub element are formed by modifying the height, width, length, cross section, and number of stub elements, and by adding additional structures to the basic stub element. Unlike a typical resonant high-Q radiator such as a dipole, slot, or patch, the CTS stub exhibits a very low-Q impedance characteristic.

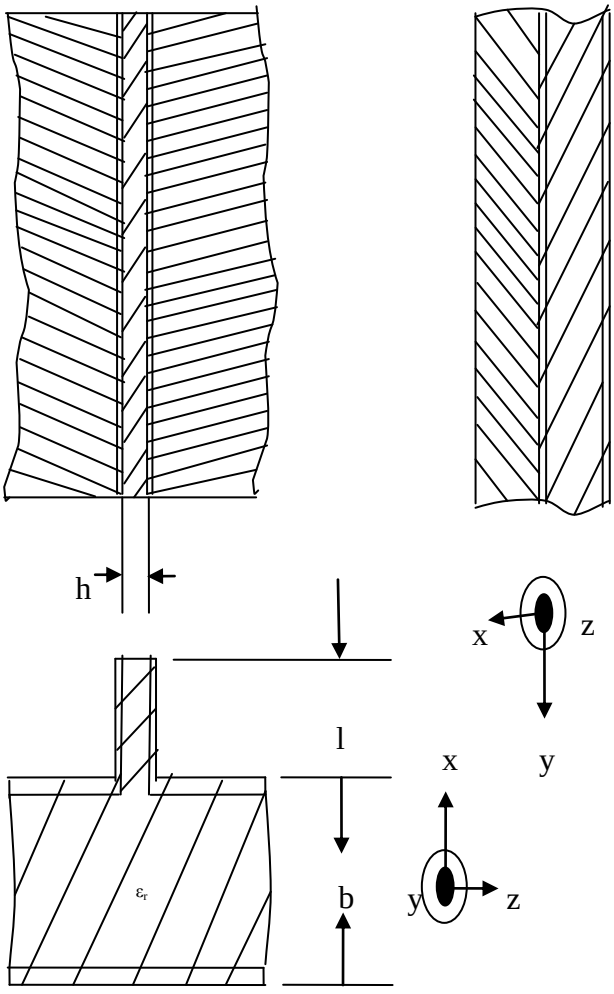

Fig. 1 Radiating CTS Element

CTS array antenna exploits a unique stub element as its radiator basis. The canonical architecture of a typical CTS antenna radiating unit is illustrated in Fig.1. The unit cell continuous transverse stub (CTS) has a width *b* and height *h* producing over the ground plane and the dielectric constant of the spacing between two stubs is $\varepsilon_{r.}$ Antenna element coupling is accomplished through variation of longitudinal stub length, stub height, parallel-plate separation, and the properties of the parallel plate and stub dielectric medium.

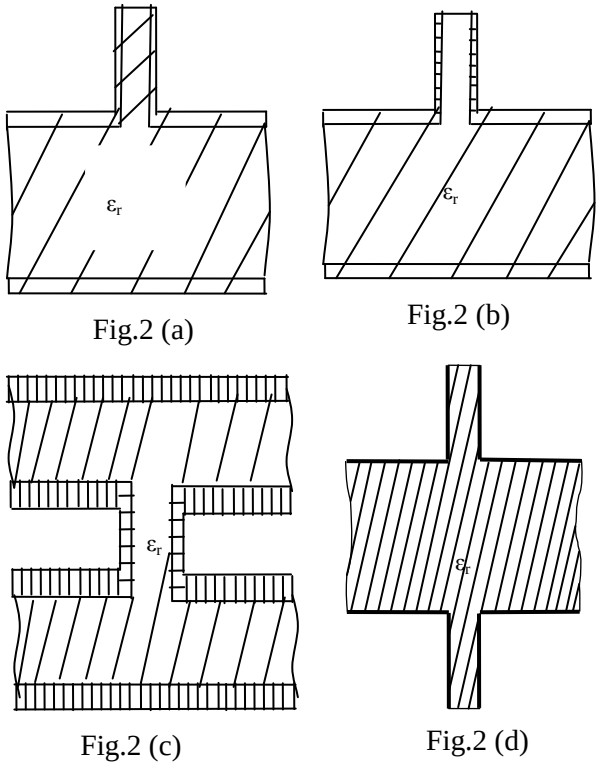

Fig.2 (a) Fig.2 (b)

Fig.2 (c) Fig.2 (d)

Fig. 2 a) Reactive CTS element (short) b)Reactive CTS element (open) c) Coupling CTS Element d) Two side CTS element

The coupling capacitance of the stub can compensate the inductance of the purely reactive stub elements, so the reflection coefficient of the unit over a range of operating frequency depends on the width of stub, the element-to-element spacing and dielectric constant of filled dielectric material. The basic two parallel plate radial stub CTS structure is depicted in Fig.3. The gap between two plates is filled with dielectric material. In this design the dielectric material used is Teflon because of its high efficiency and availability and more economic. Fig.4 depicts the already existing lengthy CTS antenna structure. This can be modified using physical dimension alteration method and it is

shown in Fig.5. Table 1 shows the dimensions of proposed CTS antenna structure. From table the observation made is in the already existing model size can be reduced 5 times to achieve the desired multiband operation.

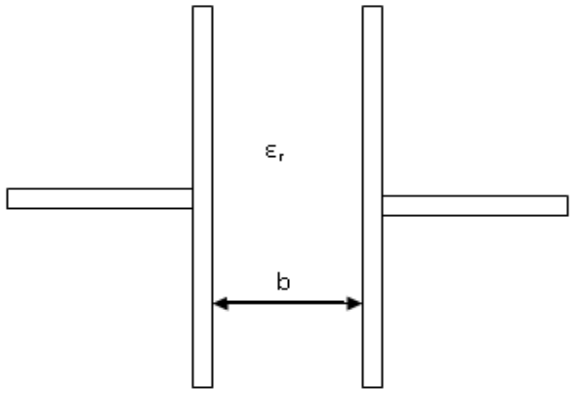

Fig. 3 Structure of two element CTS

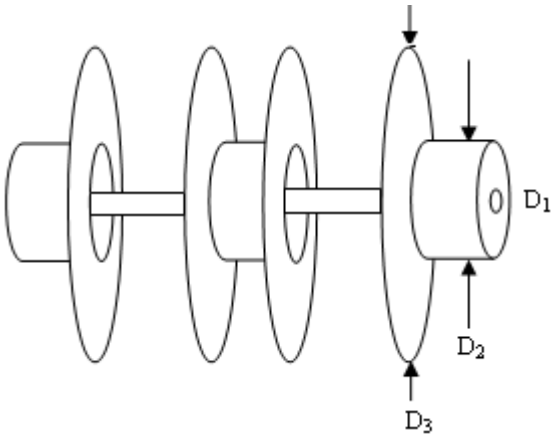

Fig. 4 Normal CTS Antenna Structure

In general coaxial CTS antenna consists of several stub elements, and each stub element includes cascade sections of standard coaxial transmission line and open-ended radiating stubs. The structure is fed by coaxial line, and the other end is connected with a matching load. There are some important parameters for coaxial CTS antenna: 1) width of stub segment L_1; 2) length of transmission line segment between stubs L_2; 3) diameter of inner conductor D_1; 4) diameter of outer conductor D_2; 5) diameter of stub D_3; and 6) dielectric constant of fill material ε_r Diameter of inner and outer conductors of the coaxial transmission line could be adjusted to obtain the desired impedance. According to transmission line theory, the impedance of coaxial line is,

$$Z0 = \frac{60}{\sqrt{\varepsilon}} \ln\left(\frac{D2}{D1}\right) \qquad (1)$$

Once the dielectric is selected, the impedance can be determined by the ratio between D_1 and D_2. In most design, 50Ω or 75Ω coaxial line is required because of the extensive use in Engineering, therefore the antenna design could be predigest. Normally the width of stubs L_1 is selected to be approximately half wave length in dielectric that fills the stub. The length of transmission line between two stubs L_2 is chosen to fulfill the phase difference so that the interference of waves radiated from stubs is rational to generate expected radiation pattern and gain.

Table 1 Dimensions of proposed CTS Antenna

Component	Material Used	Dimension
Diameter of the stub (D_3)	Brass	35mm
Stub thickness		0.5 mm
Distance between Outer conductor and stub		5mm
Length of inner conductor		36mm
Diameter of outer conductor	Brass	7mm
Diameter of inner conductor	Brass	3mm
Total length of the proposed CTS antenna array		36mm

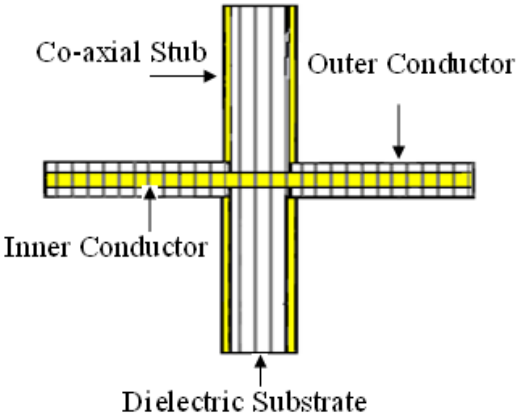

Fig. 5 (a)

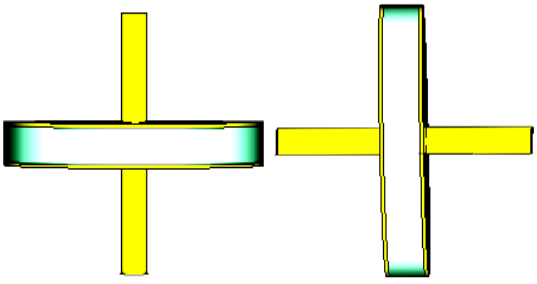

Fig. 5 (b) Fig.5 (c)

Fig. 5 Structure of proposed CTS antenna a) Cross section b) Front view c) Side view

The total length of CTS antenna is sum of length of low-frequency array [5], [6], high-frequency array and the distance between two arrays. The total length of CCTS antenna array can be calculated using the equation (2).

$$\mathbf{L = L_1 * n + L_2 * (n-1)} \quad (2)$$

3 FDTD Analysis

The Numerical analysis of this antenna structure is carried out using Finite Differential Time Domain Analysis (FDTD). Computational electromagnetic or computational electrodynamics or electromagnetic modeling [1], [2] is the process of modeling the interaction of electromagnetic fields with physical objects and the environment. It typically involves using computationally efficient approximations to Maxwell's equation and is used to calculate antenna performance like electromagnetic compatibility. A specific part of computational electromagnetic deals with electromagnetic radiation scattered and absorbed by small particles. Finite Difference Time Domain (FDTD) method [22] is a popular computational electromagnetic (CEM) technique. It is easy to understand and easier to implement in software than either finite element or method of moments. The FDTD method is attractive due to its generality, ease of implementation, linear scaling in execution time with problem size, and ability to handle dispersive and nonlinear materials. FDTD often has the best performance when analyzing structures with three-dimensional material variation [21]. The algorithm used for FDTD simulation is known as Yee algorithm [1], [2], [22].

The features of Yee Algorithm are it has spatial offset, use leapfrog time stepping technique to brought E and H offset time by half a time step as well as to avoid problems involved with simultaneous equations and matrix inversions and finite difference equations for space and time derivatives are central difference and second order accurate. In this paper proposed the modified Yee's scheme, the computational space is subdivided by using an orthogonal mesh in spherical coordinates. The electric fields are located along the edges of the cells, while the magnetic fields are positioned at the centers of these cells. In order to study antenna matching and pulse fidelity in the time domain, any spurious reflections had to be eliminated using suitable absorbing boundary conditions (ABC). The problem using spherical coordinates, the absorbing boundary layer should be spherically symmetric. The purpose of the Perfectly Matched Layer (PML) is to simulate an infinite simulation space, that is, outgoing waves are absorbed by the PML and cannot reflect back into simulation space. A unique feature of the PML is that plane waves of arbitrary incidence, polarization and frequency are matched at the boundary in a reflection less manner. The boundary of the computational space must be sufficiently far from the antenna, usually in a distance at least ten times the free space operating wavelength. The following steps explain the FDTD procedure to calculate the required antenna parameters:

Step 1: Derivation of the Field Equations for E & H

$$\overline{\nabla}\times\overline{E} = -\mu_0\frac{\partial\overline{H}}{\partial t} - Jm, \quad \overline{\nabla}\times\overline{H} = \varepsilon\frac{\partial\overline{E}}{\partial t} + Je \quad (3)$$

$$\boldsymbol{B} = \mu\boldsymbol{H}, \qquad \boldsymbol{D} = \varepsilon\boldsymbol{E} \quad (4)$$

$$\boldsymbol{J}_e = \sigma\boldsymbol{E}, \qquad J_m = \sigma^* E \quad (5)$$

Step2: Expanding Maxwell's equation in cylindrical coordinate system

$$\overline{\nabla}\times\overline{\boldsymbol{E}} = \frac{1}{\boldsymbol{r}}\begin{vmatrix} \overline{\mathbf{a}_r} & \mathbf{r}\overline{\mathbf{a}_\phi} & \overline{\mathbf{a}_z} \\ \frac{\partial}{\partial \mathbf{r}} & \frac{\partial}{\partial \boldsymbol{\phi}} & \frac{\partial}{\partial \mathbf{z}} \\ \mathbf{H}_r & \mathbf{r}\mathbf{H}_\phi & \mathbf{H}_z \end{vmatrix}$$

$$\overline{\nabla}\times\overline{E} = \overline{a_r}\left[\frac{\partial H_z}{\partial\phi} - \frac{\partial H_\phi}{\partial z}\right] - \overline{a_\phi}\left[\frac{\partial H_z}{\partial r} - \frac{\partial H_r}{\partial z}\right] - \overline{a_z}\left[\frac{\partial H_\phi}{\partial r} - \frac{\partial H_r}{\partial\phi}\right] \quad (6)$$

Equating vector components on both sides of equation (6),

$$\varepsilon\frac{\partial\overline{E_r}}{\partial t} = \frac{1}{r}\frac{\partial H_z}{\partial\phi} - \frac{\partial H_\phi}{\partial z} - \sigma E \quad (7)$$

$$\varepsilon\frac{\partial\overline{E_\phi}}{\partial t} = \frac{\partial H_r}{\partial z} - \frac{\partial H_z}{\partial r} - \sigma E \quad (8)$$

$$\varepsilon\frac{\partial\overline{E_z}}{\partial t} = \frac{1}{r}\left[\frac{\partial H_\phi}{\partial r} - \frac{\partial H_r}{\partial\phi}\right] - \sigma E \quad (9)$$

$$\overline{\nabla}\times\overline{\boldsymbol{H}} = \frac{1}{\boldsymbol{r}}\begin{vmatrix} \overline{\mathbf{a}_r} & \mathbf{r}\overline{\mathbf{a}_\phi} & \overline{\mathbf{a}_z} \\ \frac{\partial}{\partial \mathbf{r}} & \frac{\partial}{\partial \boldsymbol{\phi}} & \frac{\partial}{\partial \mathbf{z}} \\ \mathbf{E}_r & \mathbf{r}\mathbf{E}_\phi & \mathbf{E}_z \end{vmatrix}$$

$$\overline{\nabla}\times\overline{H} = \frac{1}{r}\overline{a_r}\left[\frac{\partial E_z}{\partial\phi} - r\frac{\partial E_\phi}{\partial z}\right] - \overline{a_\phi}\left[\frac{\partial E_z}{\partial r} - \frac{\partial E_r}{\partial z}\right] - \frac{1}{r}\overline{a_z}\left[r\frac{\partial E_\phi}{\partial r} - \frac{\partial E_r}{\partial\phi}\right] \quad (10)$$

Equating vector components on both sides of equation (10),

$$-\mu_0\frac{\partial\boldsymbol{H}_r}{\partial\boldsymbol{t}} = \frac{1}{\boldsymbol{r}}\frac{\partial\boldsymbol{E}_z}{\partial\boldsymbol{\phi}} - \frac{\partial\boldsymbol{E}_\phi}{\partial\boldsymbol{z}} + \sigma^*\boldsymbol{E} \quad (11)$$

$$-\mu_0 \frac{\partial H_\phi}{\partial t} = \frac{\partial E_r}{\partial z} - \frac{\partial E_z}{\partial r} + \sigma * E \tag{12}$$

$$-\mu_0 \frac{\partial H_z}{\partial t} = \frac{1}{r}\left[\frac{\partial}{\partial r}(rE_\phi) - \frac{\partial E_r}{\partial \phi}\right] + \sigma * E \tag{13}$$

Step 3: The scalar equations must be converted into FDTD equations to enable iterative time stepping. The FDTD equations are found by referring to the unit cell using the spherical, central finite difference equations Central Difference approximation Formula,

$$\frac{\partial F^n}{\partial t}(i,j,k) = \frac{F^{n+\frac{1}{2}}(i,j,k) - F^{n-\frac{1}{2}}(i,j,k)}{\ln\left(b/a\right)} + O\left(\partial t^2\right) \tag{14}$$

$$\frac{\partial F^n}{\partial t}(i,j,k) = \frac{F^n(i+1/2,j,k) - F^n(i-1/2,j,k)}{\ln\left(b/a\right)} + O\left(\partial t^2\right) \tag{15}$$

$$\frac{\partial F^n}{\partial t}(i,j,k) = \frac{F^n(i,j+1/2,k) - F^n(i,j-1/2,k)}{\ln\left(b/a\right)} + O\left(\partial t^2\right) \tag{16}$$

$$\frac{\partial F^n}{\partial t}(i,j,k) = \frac{F^n(i,j,k+1/2) - F^n(i,j,k-1/2)}{\ln\left(b/a\right)} + O\left(\partial t^2\right) \tag{17}$$

Equation (14) to Equation (17) represents the time, radial, azimuthal and height derivatives. Applying these equations to the general E and H field equations to find out the solution of proposed antenna structure and the resultant field equations are,

$$H_r\Big|_{i+\frac{1}{2},j,k}^{n+\frac{1}{2}} = D_a H_r\Big|_{i+\frac{1}{2},j,k}^{n-\frac{1}{2}} + D_{b1} \left[\begin{array}{l} E_\phi\Big|_{i+\frac{1}{2},j+\frac{1}{2},k}^{n+\frac{1}{2}} - E_\phi\Big|_{i+\frac{1}{2},j-\frac{1}{2},k}^{n+\frac{1}{2}} - \\ \dfrac{\left[E_z\Big|_{i+\frac{1}{2},j,k+\frac{1}{2}}^{n+\frac{1}{2}} - E_z\Big|_{i+\frac{1}{2},j,k-\frac{1}{2}}^{n+\frac{1}{2}}\right]}{r} \end{array}\right] \tag{18}$$

$$H_\phi\Big|_{i,j+\frac{1}{2},k}^{n+\frac{1}{2}} = D_a H_\phi\Big|_{i,j+\frac{1}{2},k}^{n-\frac{1}{2}} + D_{b1} \left[\begin{array}{l} E_r\Big|_{i+\frac{1}{2},j+\frac{1}{2},k}^{n+\frac{1}{2}} - E_r\Big|_{i-\frac{1}{2},j+\frac{1}{2},k}^{n+\frac{1}{2}} - \\ E_z\Big|_{i,j+\frac{1}{2},k+\frac{1}{2}}^{n+\frac{1}{2}} - E_z\Big|_{i,j-\frac{1}{2},k+\frac{1}{2}}^{n+\frac{1}{2}} \end{array}\right] \tag{19}$$

$$H_z\Big|_{i,j,k+\frac{1}{2}}^{n+\frac{1}{2}} = \frac{1}{r}\left[\begin{array}{l} D_a H_z\Big|_{i,j,k+\frac{1}{2}}^{n-\frac{1}{2}} + D_{b2} \\ \left[\begin{array}{l} E_r\Big|_{i,j+\frac{1}{2},k+\frac{1}{2}}^{n+\frac{1}{2}} - E_r\Big|_{i,j+\frac{1}{2},k-\frac{1}{2}}^{n+\frac{1}{2}} - \\ r\left[E_\phi\Big|_{i+\frac{1}{2},j+\frac{1}{2},k}^{n+\frac{1}{2}} - E_\phi\Big|_{i-\frac{1}{2},j+\frac{1}{2},k}^{n+\frac{1}{2}}\right] \end{array}\right] \end{array}\right] \tag{20}$$

$$E_r\Big|_{i+\frac{1}{2},j,k}^{n+\frac{1}{2}} = C_a E_r\Big|_{i+\frac{1}{2},j,k}^{n-\frac{1}{2}} + C_{b1} \left[\begin{array}{l} H_\phi\Big|_{i+\frac{1}{2},j+\frac{1}{2},k}^{n+\frac{1}{2}} - H_\phi\Big|_{i+\frac{1}{2},j-\frac{1}{2},k}^{n+\frac{1}{2}} - \\ \dfrac{H_z\Big|_{i+\frac{1}{2},j,k+\frac{1}{2}}^{n+\frac{1}{2}} - H_\phi\Big|_{i+\frac{1}{2},j,k-\frac{1}{2}}^{n+\frac{1}{2}}}{r} \end{array}\right] \tag{21}$$

$$E_\phi\Big|_{i,j+\frac{1}{2},k}^{n+\frac{1}{2}} = C_a E_\phi\Big|_{i,j+\frac{1}{2},k}^{n-\frac{1}{2}} + C_{b2} \left[\begin{array}{l} H_r\Big|_{i+\frac{1}{2},j+\frac{1}{2},k}^{n+\frac{1}{2}} - H_r\Big|_{i-\frac{1}{2},j+\frac{1}{2},k}^{n+\frac{1}{2}} - \\ H_z\Big|_{i,j+\frac{1}{2},k+\frac{1}{2}}^{n+\frac{1}{2}} - H_\phi\Big|_{i,j-\frac{1}{2},k+\frac{1}{2}}^{n+\frac{1}{2}} \end{array}\right] \tag{22}$$

$$E_z\Big|_{i,j,k+\frac{1}{2}}^{n+\frac{1}{2}} = \frac{1}{r}\left[\begin{array}{l} C_a E_z\Big|_{i,j,k+\frac{1}{2}}^{n-\frac{1}{2}} + C_{b3} \\ \left[\begin{array}{l} H_r\Big|_{i,j+\frac{1}{2},k+\frac{1}{2}}^{n+\frac{1}{2}} - H_r\Big|_{i,j+\frac{1}{2},k-\frac{1}{2}}^{n+\frac{1}{2}} - \\ r\left[H_\phi\Big|_{i+\frac{1}{2},j+\frac{1}{2},k}^{n+\frac{1}{2}} - H_\phi\Big|_{i-\frac{1}{2},j+\frac{1}{2},k}^{n+\frac{1}{2}}\right] \end{array}\right] \end{array}\right] \tag{23}$$

Where,

$$C_a = \frac{1 - \dfrac{\sigma_{i,j,k}.\Delta t}{2\varepsilon_{i,j,k}}}{1 + \dfrac{\sigma_{i,j,k}.\Delta t}{2\varepsilon_{i,j,k}}} \tag{24}$$

$$C_{b1} = \frac{\dfrac{\Delta t}{\varepsilon_{i,j,k,\Delta 1}}}{1 + \dfrac{\sigma_{i,j,k}.\Delta t}{2\varepsilon_{i,j,k}}} \tag{25}$$

$$C_{b2} = \frac{\dfrac{\Delta t}{\varepsilon_{i,j,k,\Delta 2}}}{1 + \dfrac{\sigma_{i,j,k}.\Delta t}{2\varepsilon_{i,j,k}}} \tag{26}$$

$$D_a = \frac{1 - \dfrac{\sigma_{i,j,k}.\Delta t}{2\varepsilon_{i,j,k}}}{1 + \dfrac{\sigma_{i,j,k}.\Delta t}{2\varepsilon_{i,j,k}}} \tag{27}$$

$$D_b = \frac{\dfrac{\Delta t}{\varepsilon_{i,j,k,\Delta 2}}}{1 + \dfrac{\sigma_{i,j,k}.\Delta t}{2\varepsilon_{i,j,k}}} \tag{28}$$

Step 4: Driving Signal

The base of the antenna is driven by a voltage signal through a coaxial line. The coaxial line has an inner conductor diameter "a" and an outer conductor diameter "b". The voltage on the coaxial line is a solution to the wave equation in cylindrical coordinates

$$\frac{1}{r}\frac{\partial}{\partial r}\left(r\frac{\partial V}{\partial r}\right) + \frac{1}{r^2}\frac{\partial^2}{\partial \theta^2} = 0 \tag{29}$$

Note that the θ units of this equation are different from the θ units of the spherical coordinates of the antenna. This equation is subject to the boundary conditions V(a, θ) = V_o and V(b, θ) =0. In actuality, V_o will vary with time, but the time variation can be introduced once the static solution is found. Since the coaxial line is axially symmetric, the solution is independent of θ . The wave equation in cylindrical coordinates simplifies to,

$$\frac{1}{r}\frac{\partial V}{\partial r}\left(r\frac{\partial V}{\partial r}\right)=0 \tag{30}$$

This has the general solution

$$V(r,\theta)=C.\ln(r)+D \tag{31}$$

Applying the boundary conditions gives the final solution for the coaxial driving voltage

$$V(r,\theta)=V_0.\frac{\ln(r/b)}{\ln(b/a)} \tag{32}$$

4 Results and Discussion

The 3D electromagnetic simulation software package CST Microwave Studio is used to simulate the coaxial CTS antenna array structure. Fig.6 and Fig.7 shows the field and VSWR plot of single stub CTS antenna using modified FDTD based simulation which shows that it produces omni directional radiation pattern in the horizontal plane for desired VSWR. Table.2. shows the extracted parameters of proposed CTS antenna structure. The proposed structure radiates for 5 bands of frequencies with very good S-parameter (S_{11}) and Omni directional pattern for all bands shown in Fig.8 and Fig11 to Fig.18. Fig.9 and Fig.10 shows the power delivered and EMC plot of proposed antenna structure. These plots show that the antenna should radiate with minimum power and EMC compatible. These parameters should be tabulated in Table 2. Table 2 shows the extracted parameters of proposed CTS antenna structure. Thse results shows that the two element CTS antenna produces very good gain and low tanloss and minimum loss. From Table 2 the observation made is the five band of frequencieds are suitable for satellite K band and Ka band applications. These results are compared with already existing models [5], [6], [8], [10] and [11]. From these results the proposed model is well miniaturized to operate for multiple band of frequencies.The power delivered is very less so that this natenna is well suitable for low power applications. The loss tangent is a parameter of a dielectric material that quantifies its inherent dissipation of electromagnetic energy. The term refers to the tangent of the angle in a complex plane between the resistive (lossy) component of an electromagnetic field and its reactive (lossless) component. Table 1 show that the tan loss of proposed structure has very less compared to other structures.

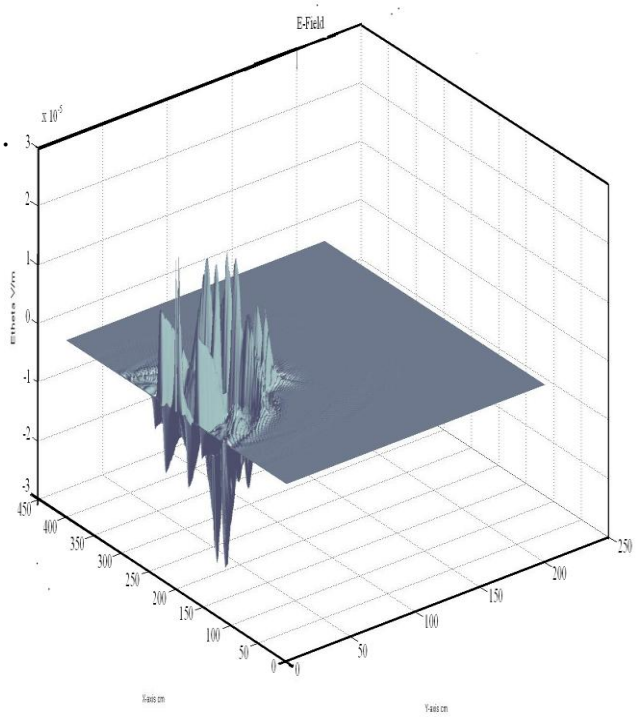

Fig.6. E-field pattern of Single Stub radiating element.

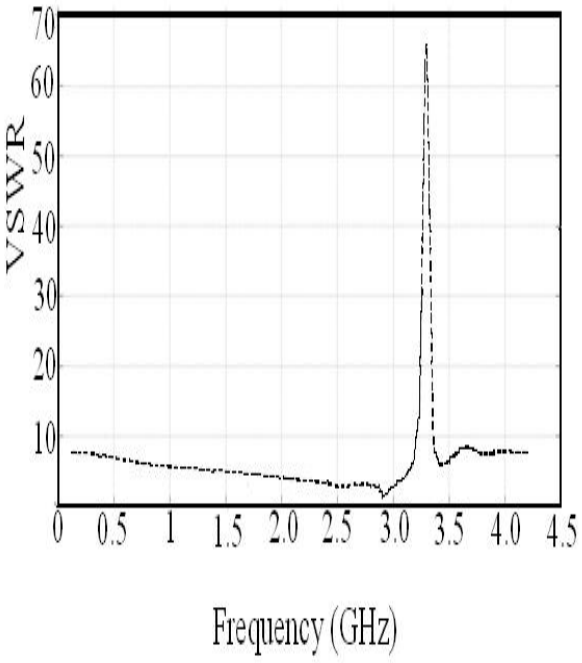

Fig.7. VSWR plot of single radiating stub.

Table 2 Extracted parameters of proposed CTS Antenna

Frequency (GHz)	Skin Depth (μm)	Loss Angle	S_{11} (dB)	VSWR	P_{max} (dBW/m^2)	D (dBi)	G (dB)	E-Field (dBV /m^2)	H-Field (dBA/m)
23	0.44	0.01	-24.14	1:1.132	-6.207	5.509	4.940	19.55	-31.97
25.5	0.41	0.01	-17.01	1:1.329	-9.173	1.558	1.558	16.59	-34.93
27	0.40	0.01	-21.64	1:1.181	-9.076	1.432	1.958	16.69	-34.85
29	0.39	0.01	-21.42	1:1.186	-8.893	1.677	2.105	16.86	-34.65
31.5	0.37	0.01	-39.82	1:1.021	-9.844	0.639	1.162	15.92	-35.604

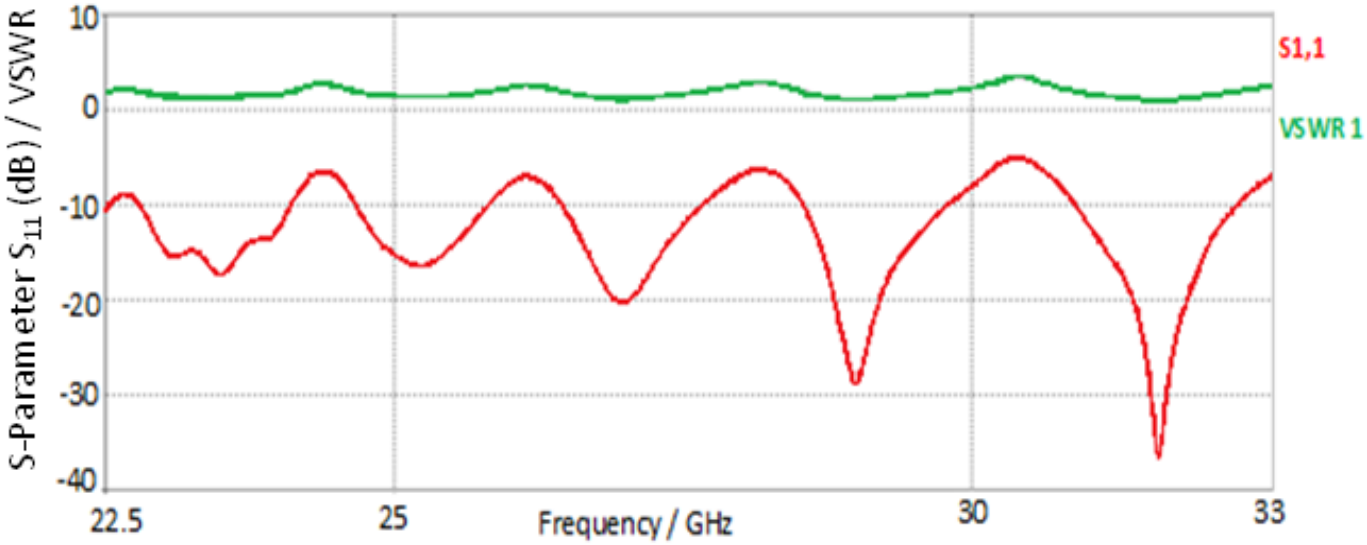

Fig.8 S-Parameter (S_{11} and VSWR plot of proposed Continuous Transverse Stub antenna

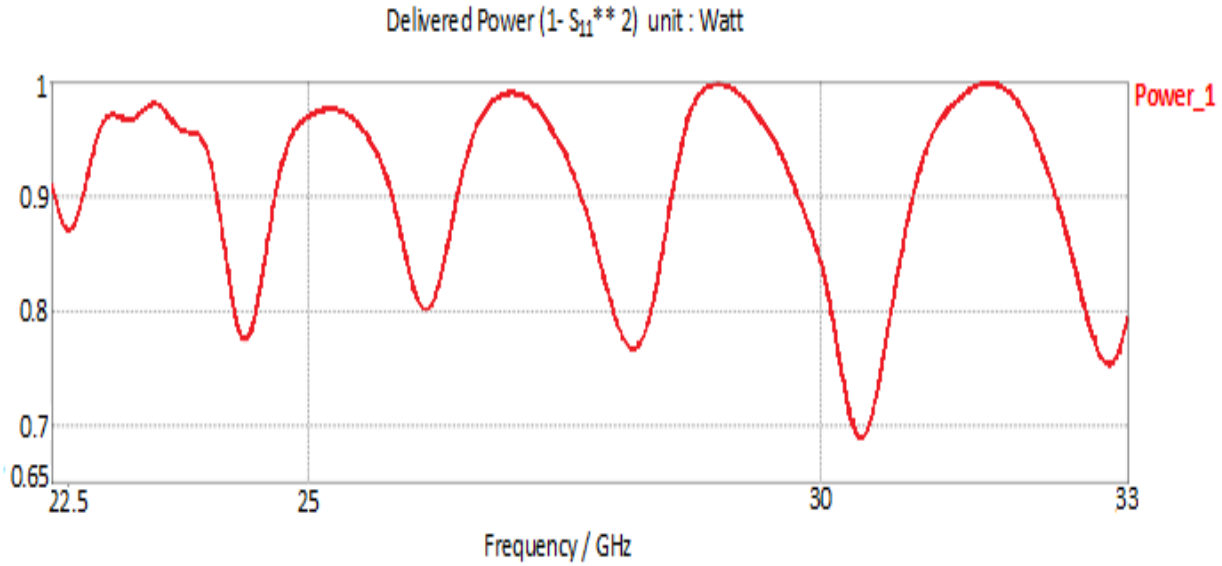

Fig.9. Delivered power plot of proposed Continuous Transverse Stub antenna

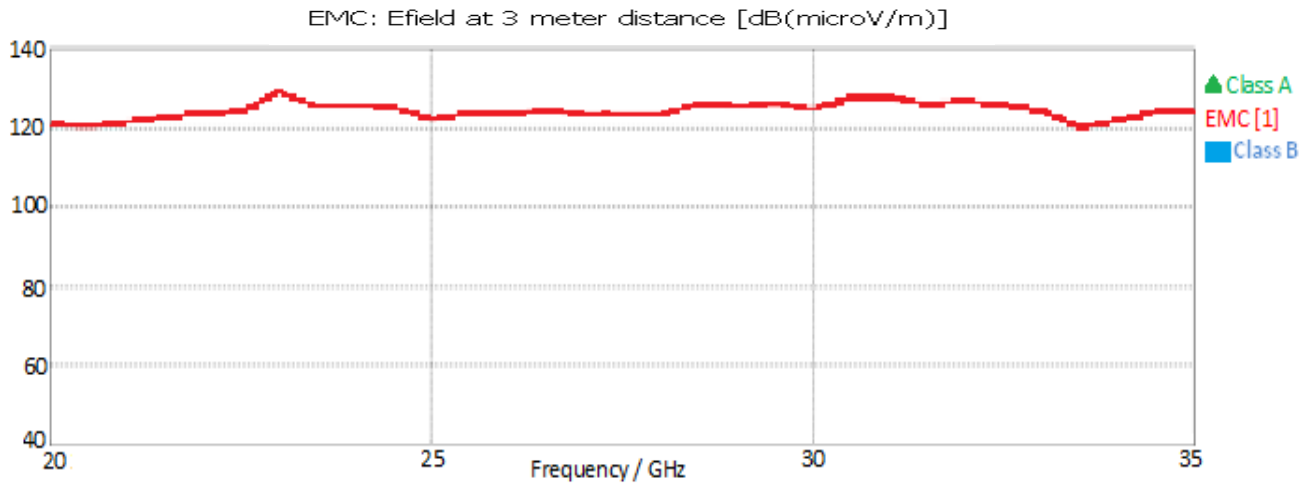

Fig.10. EMC plot of proposed Continuous Transverse Stub antenna

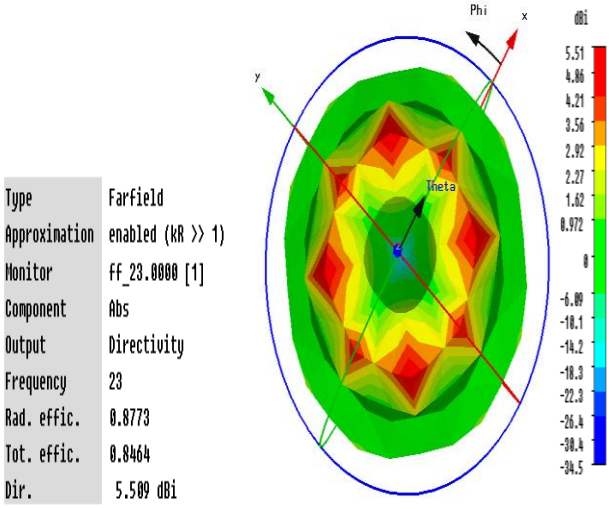

Fig. 11 (a)

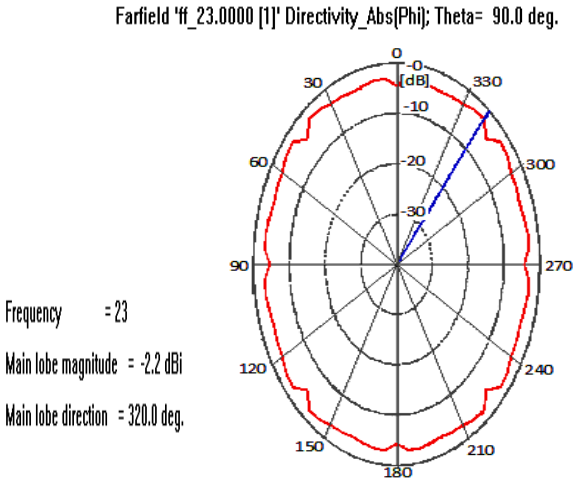

Fig. 11 (b)

Fig.11.Radiation pattern of Continuous Transverse Stub antenna at 23 GHz a) 3-D b) 2-D

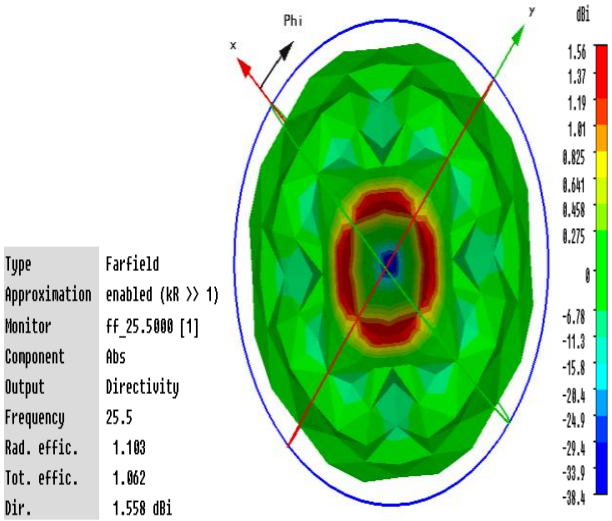

Fig. 12 (a)

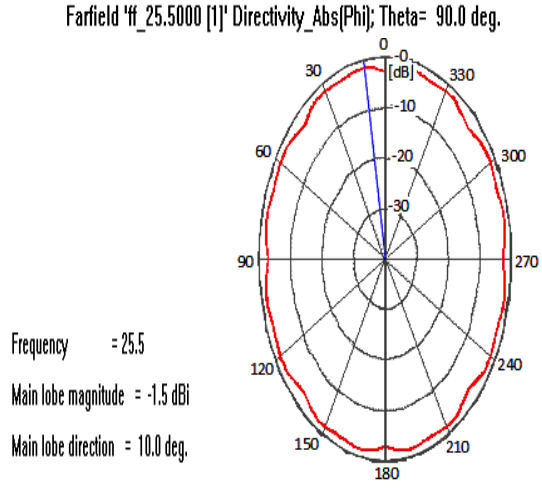

Fig. 12 (b)

Fig.12.Radiation pattern of Continuous Transverse Stub antenna at 25.5 GHz a) 3-D b) 2-D

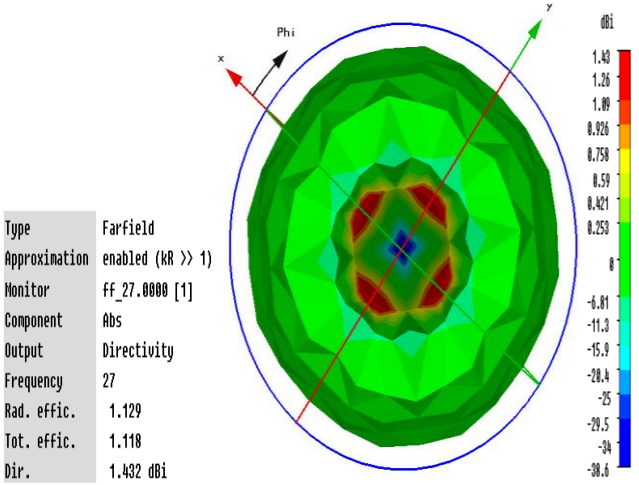

Fig. 13 (a)

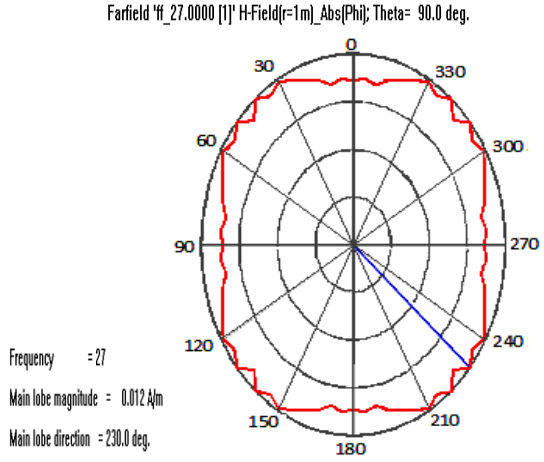

Fig. 13 (b)

Fig.13.Radiation pattern of Continuous Transverse Stub antenna at 27 GHz a) 3-D b) 2-D

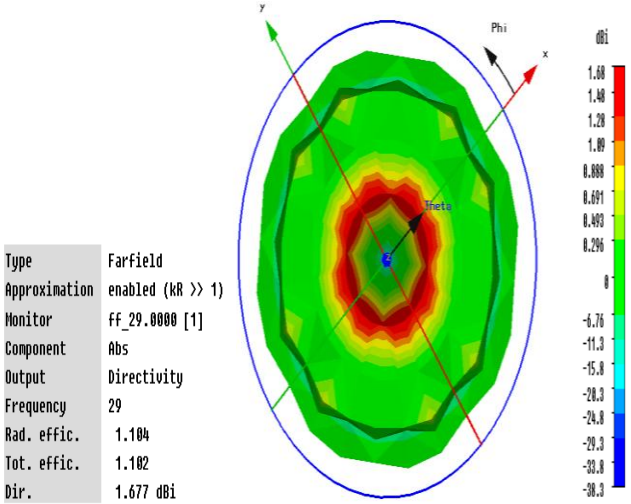

Fig. 14 (a)

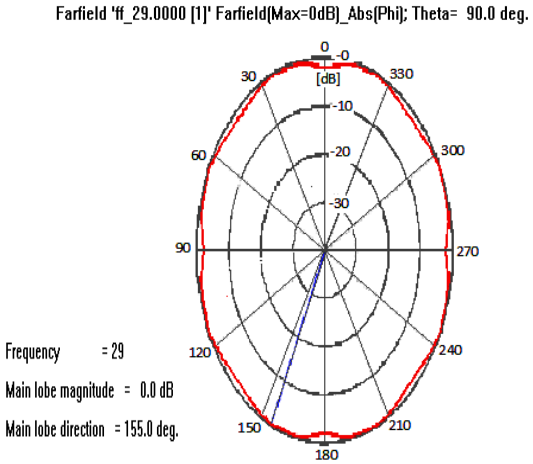

Fig. 14 (b)

Fig.14.Radiation pattern of Continuous Transverse Stub antenna at 29 GHz a) 3-D b) 2-D

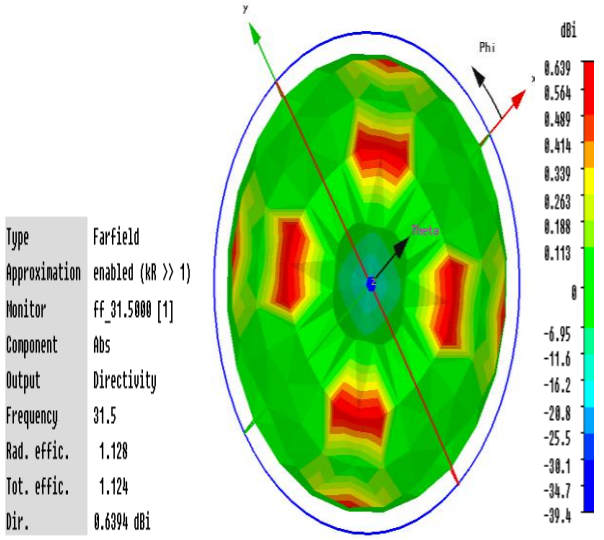

Fig. 15 (a)

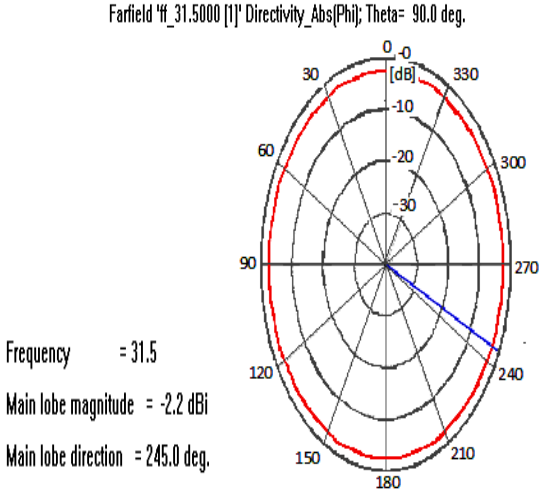

Fig. 15 (b)

Fig.15. Radiation pattern of Continuous Transverse Stub antenna at 31.5 GHz a) 3-D b) 2-D

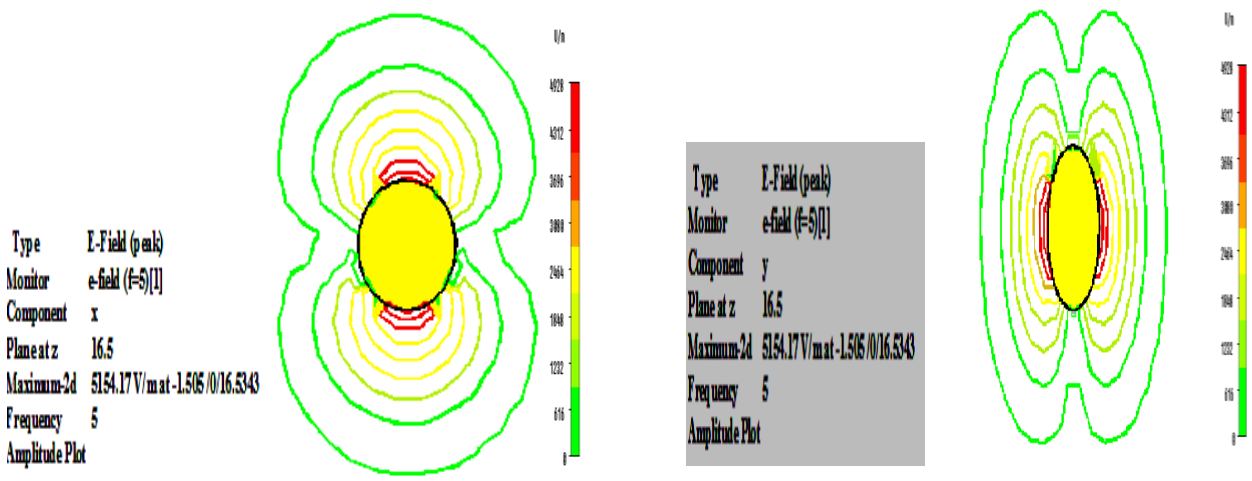

Fig.16. E-field port mode X and Y direction plot of proposed Continuous Transverse Stub antenna

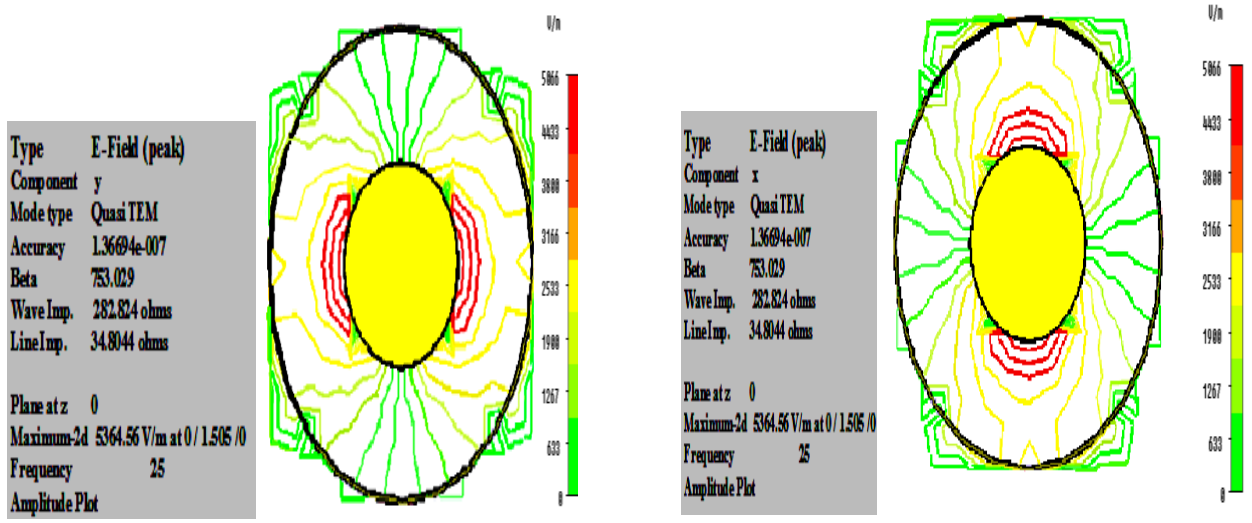

Fig.17. E-field normal X and Y direction plot of proposed Continuous Transverse Stub antenna

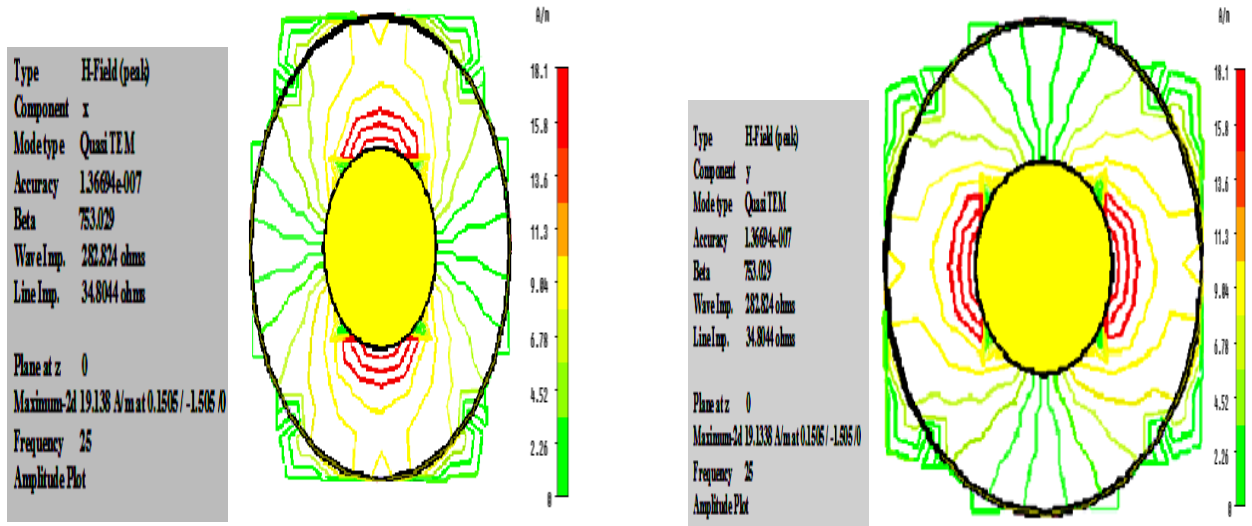

Fig.18. H-field normal X and Y direction plot of proposed Continuous Transverse Stub antenna

5 Conclusion

As far as the objective is concerned, design and analysis of a number of basic available models [1],[2],[5],[16], [20] were designed and their results were analyzed. From the results obtained and depending on the need of the present wireless communication systems number of novel indigenous models have been designed. From these models it can be judged that almost similar parametric operations are obtained. To design the antenna with two elements is used to Improve the radiation pattern, bandwidth and reduces side lobe level. Thus the need for different designs for multi band operations got eliminated. Various structures can be fine-tuned to get optimum results in future. This proposed structure S-parameter and radiation shows that the operating frequency of the antenna is well suited for satellite K-band and Ka-Band transmitting and receiving purpose. This can be implemented in practically in future.

6 Acknowledgment

I thank my research guide Dr.(Mrs) S.Raju for her support and valuable suggestion for the successful completion of my research work. I thank my husband and sons for their support and encouragement for succeeding my research work in a stipulated time. I thank god almighty to succeed my level for the successful completion and submission of this research work in WSEAS Journal.

References:

[1] K. S. Yee, "Numerical solution of initial boundary value problems involving Maxwell´s equations in isotropic media," *IEEE Trans. Antenna and Propagation*. vol.14, pp. 302-307, 1966.

[2] S.Q.Xiao, Z.H. Shao, and B.Z. Wang , "Application of Improved Matrix Type FDTD Method For Active Antenna Analysis", *Progress In Electromagnetic Research*, pp. 245- 263,2010.

[3] Iskander. M.F, Kim .W, Bell. J, Celik .N, Zhengqing Yun and Hyoung-sun Youn, "Antenna Arrays Technologies for advanced wireless systems", *IEEE International Conference on Microwaves, Communications, Antennas and Electronics Systems (COMCAS 2009)*, pp.1-4, 2009.

[4] Seung-Yeup Hyun, Se-Yun Kim , and Young-Sik Kim, "An Efficient FDTD Model for Resistively Loaded Cylindrical Antennas With Coaxial Lines", *IEEE Transactions on Antennas and Propagation*, vol.57, no. 2, pp.484 – 490, 2009.

[5] Bo Sun, Jinghui Qiu, Lingling Zhong and Xiaohang Xing, "Design of Double Frequency Coaxial CTS antenna", *Progress In Electromagnetics Research Symposium, Hangzhou, China*, pp.875-877,2008.

[6] W. Kim, M. Iskander, and C. Krowne, "Modified Green's Function and Spectral Domain Approach for Analyzing Anisotropic and Multi-Dielectric Layers Coplanar Waveguide Ferroelectric Phase Shifters", *IEEE transactions on Microwave Theory and Techniques*, vol. 55, pp. 402-409, 2007.

[7] J. M. Bell and M. F. Iskander, "Ultrawideband Hybrid EBG/Ferrite Ground Plane for Low-Profile Array Antennas", *IEEE Transactions on Antennas and Propagation*, vol. 55, pp.4-12, 2007.

[8] Iskander, M.F., Zhengqing Yun Celik, N. Bell and J. Kim, "Antenna Arrays and Propagation Models for Advanced Wireless Systems*", IEEE International Conference on Electromagnetics in Advanced Applications ICEAA*, pp.79 –84,2007.

[9] Iskander M.F, Celik N, Kim. W, "Low Cost Phased Array Antennas Using Analog and Digital Phase Shifters Technologies", *IEEE Antennas and Propagation Society International Symposium*, pp.37 – 40, 9-15 , 2007.

[10] R. Isom, M. F. Iskander, Z. Yun, and Z. Zhang, "Design and development of multi- band Coaxial Continuous Transverse Stub(CTS) Antenna Arrays", *IEEE Trans. on Antennas and Propagation*, vol.52, 2180 -2184, 2004.

[11] M.F. Iskander, and Wayne Kim M.F.A,"New Coplanar Waveguide Continuous Transverse Stub (CPW-CTS) Antenna For Wireless Communications", *IEEE Antenna and Wireless Propagat. Letters*,Vol.4, pp.172-74,2005.

[12] Rezk, M, Kim. W, Zhengqing Yun, Iskander. M," Narrow Beam Adaptive Array For Advanced Wireless Applications", *IEEE/ACES International Conference on Wireless Communications and Applied Computational Electromagnetics*, pp. 594 - 597 , 2005.

[13] Iskander, M.F., Zhang, Z., Yun, Z., and Isom. R., "Coaxial Continuous Transverse Stub (CTS) Array", *IEEE Microwave and Wireless Letters*, vol.11, no. 12, pp. 489-491, 2001.

[14] R. Isom, M Iskander, Z. Zhang and Z. "Yun, "Muti-Band and Broadband Coaxial CTS Array Design", *IEEE Antennas and Propagation Society AP-S International Symposium Digest*, 2001

[15] Robert Isom, Magdy F. Iskander, Zhengqing Yun, and Zhijun Zhang, "Design and development of Multi-band Antenna Array for Multi Service Wireless Communication Networks", *Vehicular Technology Conference, pp.*58, 37-39,2003.

[16] M. Iskander, Z. Zhang and Z. Yun, "Coaxial continuous transverse stub element device antenna array and filter," *U.S. Patent 6201 509*.

[17] Mrs. P. Jothilakshmi, Dr.(Mrs.) S. Raju, "Development of Multiband Antenna for High Frequency Applications", *International Conference on Communication Technology and System* Design *2011* Elsevier Procedia Engineering 30(2012), pp.1013-1019,2012.

[18] V. P. Matterer, "Phase tuning technique for a Continuous Transverse Stub Antenna Arrays," *U.S.Patent 5 604 505.*.
[19] W. W. Milroy, "Continuous Transverse Stub Element Devices and Methods of Making Same,"*U.S. Patent 5,266,961,1991*.
[20] Jinghui Qiu, Xiaohang Xing and Lingling Zhong, "A Novel Coaxial CTS Antenna Design", *International Conference on Antenna Theory and Techniques*, Sevastopol, Ukraine pp.323-325, 2007.
[21] Umran.S.Anan and Robert.A.Marshall, "*Numerical Electromagnetics*", Second Edition.
[22] A.Taflove and S. Hangness, "Local Subcell Models of Finite Geometrical Features in Computational Electromagnetics: The Finite Difference Time-Domain Method", Second Edition. Bostan, MA:Artech House, ch.10, pp. 420 – 423, 2000.

Mrs.P.Jothilakshmi has received her B.E. degree in Electronics and Communication Engineering in Thanthai Periyar Govt. Institute of Technology, Vellore, Madras University, India in 1996 and M.E in Communication Systems in Mepco Schlenk Engineering College, Sivakasi, Madurai Kamaraj University, India in 2001. Currently working as an Assistant Professor in Electronics and Communication Engineering Department at Sri Venkateswara College of Engineering, Chennai, India. She has been a teacher for past 15 years and guided more than twenty five B.E and M.E Students. She has published more than thirty three conference and Journal papers both National and International level. Pursuing Ph.D in the area multiband antenna design under the supervision of Dr.(Mrs) S.Raju, Professor and Head, Department of Electronics and Communication Engineering, Thiagarajar College of Engineering, Madurai, India. She is a member in professional societies ISTE, IETE and IAENG.

Dr.(Mrs) S.Raju has received her B.E degree in Electronics and Communication Engineering from P.S.G college of Technology, India in the year 1982 and M.E in Communication systems in 1984 from Regional Engineering College Trichy, India. She obtained her PhD in the area of Microwave integrated circuits in the year 1996 from Madurai Kamaraj University. She was the first women engineer to obtain Ph.D from Madurai Kamaraj University. India, currently working as a Professor and Head of Department of Electronics and Communication Engineering and as a Coordinator of TIFAC CORE in Wireless Technologies at Thiagarajar College of Engineering, Madurai, India. She has been a teacher for the past twenty eight years and has successfully guided eight Ph.D scholars and currently seven scholars are pursuing PhD under her supervision. She has guided more than fifty M.E and M.S Students. She has co authored forty seven technical papers in International and National Journals. She has published sixty papers in International and National Conferences. She has successfully completed seven research projects for Defense Research Development Organization (DRDO) Laboratories, namely RCI, Hyderabad , DEAL Dehradun and ARDB, New Delhi. She has been awarded Career Award for Young Teachers in the year 1997 by AICTE, New Delhi and TCE Management Award. She has been research council member, Academic Council Member, Chairman Board of Studies of Electronics and Communication Engineering of Anna University, India.